Monatshefte für Chemie 138, 293–299 (2007)
DOI 10.1007/s00706-007-0612-7
Printed in The Netherlands

Monatshefte für Chemie
Chemical Monthly

Mechanical Properties of Organic-Inorganic Hybrid Materials Determined by Indentation Techniques

Thomas Koch[1,*], **Franz R. Kogler**[2], **Ulrich Schubert**[2], and **Sabine Seidler**[1]

[1] Institute of Materials Science and Technology, Vienna University of Technology, Vienna, Austria
[2] Institute of Materials Chemistry, Vienna University of Technology, Vienna, Austria

Received December 5, 2006; accepted (revised) January 25, 2007; published online April 6, 2007
© Springer-Verlag 2007

Summary. The mechanical properties of hybrid materials consisting of polystyrene (*PS*), which was cross-linked with different proportions of the multifunctional cluster $Zr_6O_4(OH)_4$(methacrylate)$_{12}$ (*Zr6*) were investigated. With the help of (micro)indentation and scratch testing, the influence of the *Zr6* clusters on mechanical properties, such as hardness, stiffness, creep, craze initiation, and scratch resistance was shown. There was only a slight increase in hardness and in indentation modulus with higher cluster loadings. While this observation was in agreement with the compression behaviour of the materials, the tensile properties showed a much stronger dependence on the *Zr6* content. With increasing cluster loading, an increase of craze initiation stress, as determined by ball indentation experiments, was found. Performing scratch testing with constant load, a reduction of pile-up and a stronger recovery were observed for the hybrid materials compared to the neat *PS*. Scratch tests with a constant increase of load showed an increase of the critical load for crack opening during scratching.

Keywords. Clusters; Microhardness; Polystyrene.

Introduction

The combination of organic and inorganic components at the molecular level is a challenging task in materials science and chemistry. Generally, organic-inorganic hybrid materials can be categorized into two classes: In Class I systems there are only weak interactions (no covalent or ionic bonds) between the organic and inorganic components. In Class II systems the organic and inorganic components are linked by chemical bonds. Generally, organic-inorganic materials are promising materials with improved properties compared to the organic polymers. Besides special physical properties (electrical, magnetical, optical) they may especially exhibit improved surface properties such as hardness and scratch resistance.

One sub-class of organic-inorganic hybrid materials are polymers doped with transition metal oxo-clusters with polymerizable surface ligands. The use of preformed inorganic entities as building blocks for the hybrid materials has some advantages [1]. Clusters are monodisperse with an exact defined size and shape. Most of the atoms are surface atoms and the interaction with the polymer matrix is at the maximum, and a chemical surface modification can be easily achieved [2]. Clusters can have intrinsic properties such as magnetic or optical, which could be introduced into the polymers.

Indentation testing, covering methods where an indenter is loaded and penetrates a surface, is an established tool to describe important mechanical properties of organic-inorganic hybrid materials. The thus accessible microhardness is of special interest in the characterization of organic-inorganic coatings [3–8], but also for the evaluation of bulk materials [9–11]. Besides the determination of short time hardness values, which is the normal case, there is also work dealing with creep behaviour to obtain time-dependent materials parameters [12].

* Corresponding author. E-mail: tkoch@mail.zserv.tuwien.ac.at

Modern indentation testing devices additionally offer the possibility to perform scratch tests which help describing the scratch resistance of the materials. Whereas in metals the scratch resistance correlates sufficiently well with the hardness, the problem is more difficult in the case of polymers or polymer-based materials. The scratch behaviour is influenced by a combination of hardness, viscoelasticity, and toughness. Especially the most important parameter, the (subjective) visibility of the scratches is influenced by the pile-up of the scratch edges and to a very large extent by the stress-whitening.

Results and Discussions

The inorganic-organic hybrid materials investigated in this work were prepared by free radical polymerization of varying proportions of the zirconium oxo cluster $Zr_6O_4(OH)_4(methacrylate)_{12}$ (Fig. 1) (*Zr6*) and styrene as co-monomers. About 30 g of bubble- and crack-free bulk samples of the hybrid materials were produced as previously described [13–15].

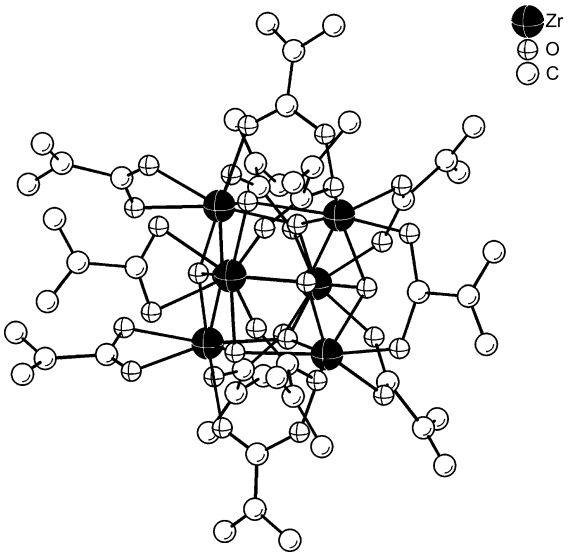

Fig. 1. Structure of $Zr_6O_4(OH)_4(methacrylate)_{12}$ (*Zr6*). The hydrogen atoms are not shown for clarity

Evaluation of Cross-Linking

The incorporation of *Zr6* clusters should lead to the formation of a permanent network in the thermoplastic polystyrene. Thus, some characteristic properties like temperature dependence of storage modulus change from typical thermoplastic to rubber-like. In Fig. 2a the storage modulus E' as a function of temperature is shown. In the temperature region below the glass transition the storage modulus of the cluster doped materials was shifted up to 20% to higher values compared to the neat *PS*. This relatively small effect was as expected, because the influence of cross-linking on the modulus of a stiff thermoplastic polymer is small in this temperature range. The increase should be caused by both, cross-linking and a (nano-)filler effect. In the glass transition region the moduli drop dramatically. For the neat *PS* it can be observed that a clear deviation from a more or less linear decrease with increasing temperature occurs at distinct lower temperatures compared to the cluster doped materials. This opens the possibility to extend the range of application of the hybrid materials to somewhat higher temperatures. Doping with the *Zr6* clusters led to the development of a rubber plateau, which was dependent on the cluster concentration in the polymer. This plateau was absent for neat *PS*. In this region the polymer chains show full segmental mobility and the properties are ruled by the entangled network [16]. The strict dependence of that

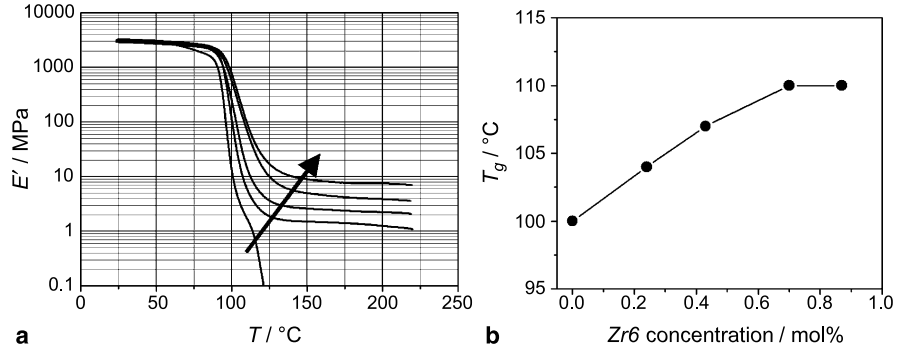

Fig. 2. Storage modulus E' as a function of temperature, the arrow indicates increasing cluster content (a) and glass transition temperature T_g as a function of cluster content (b)

rubber moduli from the cluster content proves the cross-link efficiency of the clusters. The glass transition temperatures T_g, determined at the maxima of mechanical loss, increase with cluster loading by ~10 K (Fig. 2b). That is also a measure of an increasing cross-linking with increasing *Zr6* proportion.

Quasi-Static Mechanical Behaviour

Stress–strain curves of neat *PS* and the 0.87 mol% cluster doped material are shown in Fig. 3a. Both curves show brittle materials behaviour. The tensile strength σ_m is increased to a large extend (about 60% for the material with 0.87 mol% cluster) by the addition of *Zr6*. The dependency of the tensile strength on the cluster content can be seen in the insert in Fig. 3a. Note, that the strength of neat *PS* is relatively low compared to several commercial products. This was explained with the lower molecular weight and a higher polydispersity of the laboratory product when compared to typical commercial products. The modulus of elasticity at room temperature increases from 3060 MPa (neat polymer) to 3770 MPa (0.87 mol% cluster) but this is small compared to the improvement in strength. These results indicate that the behaviour in the damage and failure region is stronger influenced by the clusters, *i.e.* the cross-linking, than the properties in the elastic deformation range. Also, the results confirm the DMA measurements, which have shown a comparable increase in storage modulus in the ambient temperature region.

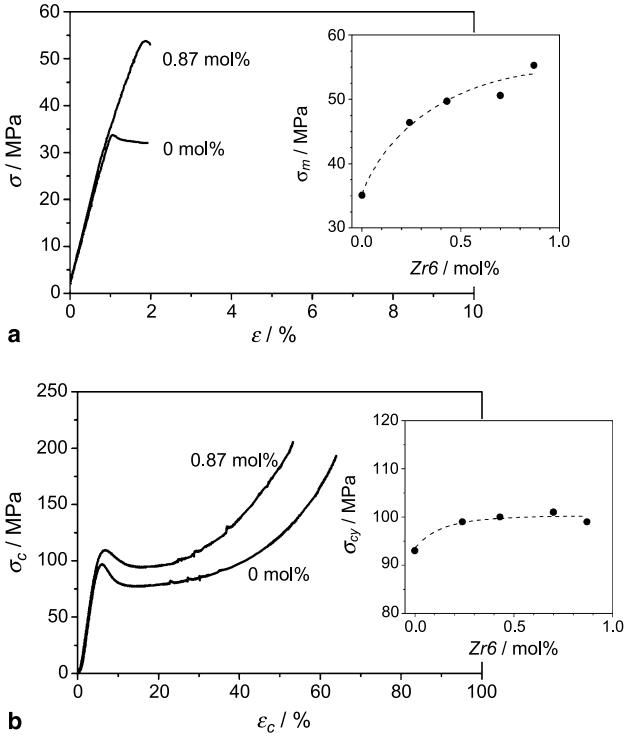

Fig. 3. Results of the tensile (a) and the compression tests (b)

The deformation behaviour in compression is completely different. Only a relatively small increase of the compression yield stress σ_{cy} was observed (Fig. 3b). Adding of *Zr6* clusters leads to a rise of 8% of the yield stress. There is practically no difference between the cluster doped materials. A comparable behaviour, only small influence of cross-linking on the compression yield stress was already described in Ref. [16] for conventionally chemical cross-linked *PS*. The compression yield stress is mainly influenced by the secondary interactions between the polymer chains and therefore largely unaffected by the cross-linking. Additionally, a decrease of strain softening, *i.e.* the drop of stress after the yield point, can be observed. In principle, the strain softening is also governed by secondary interactions. Thus, the detected behaviour can be attributed to a stabilising effect of the network [16].

Surface Properties

The indentation hardness H_{IT} increased slightly by about 10% upon doping the *PS* matrix with *Zr6* (Fig. 4). A comparable behaviour can be observed for the indentation modulus E_{IT}. The influence of the cross-linking is small. This confirms the results of the compression tests, which showed a comparable behaviour of the compression yield strength. This should originate from the similar nature of the involved deformations. The main part of the loading during a hardness test is compression and the deformation is shear dominated. Additionally, no crazing or voiding could be observed in the compression tests, and shearing dominates. In contrast, hardness does not correlate with tensile strength, a correlation which is often found. The reason for that was indicated above. The network density strongly controls the strength under tensile loading whereas hardness is less affected.

Cross-linking of thermoplastics should improve the creep behaviour [17], *i.e.* reduce the creep compliance. Indentation creep tests are a suitable method to describe the time dependent materials behaviour, especially when only small amounts of material are available as is normally the case in the first stages

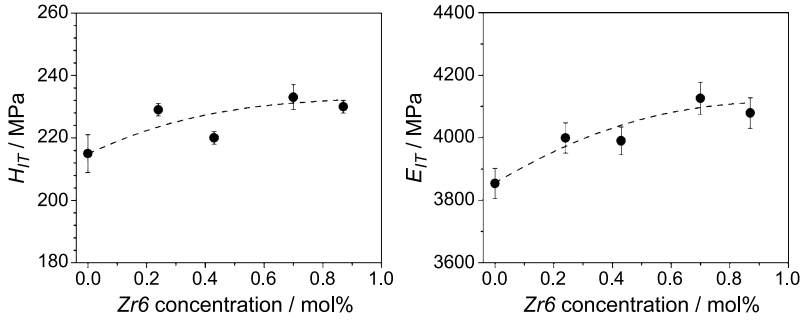

Fig. 4. Indentation hardness H_{IT} and modulus E_{IT} as a function of *Zr6* cluster content

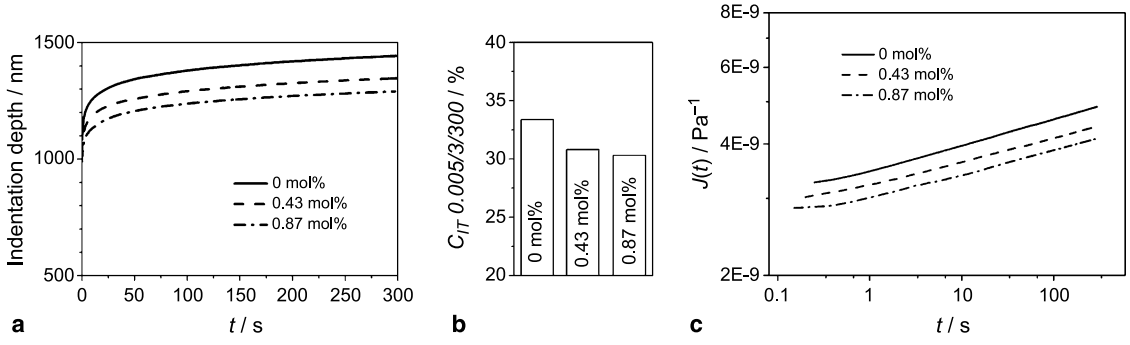

Fig. 5. Indentation creep curves (a), indentation creep parameter (b) and indentation creep compliance of *Zr6* cluster doped *PS*, spherical tip

of materials development. Typical indentation creep curves are shown in Fig. 5a. As expected for visco-elastic-viscoplastic polymers, the indentation depth increases with time when a constant load is applied to the sample over a period of time. The plot of the indentation creep parameter C_{IT} against the cluster content shows a slight decrease of creeping with increasing cluster loading (Fig. 5b). This is due to the cross-linking by the clusters irrespective of the nature of the interaction, chemical or physical. These results are reflected also by the curves of the creep compliance. Incorporating *Zr6* clusters to the *PS* matrix reduces the creep compliance of the material (Fig. 5c). The results are in the range of cross-linked epoxy resins [18]. Note, that the creep compliances determined by indentation methods are generally higher than values obtained by standard methods, *i.e.* rheometry, because the (equivalent) strains applied in the indentation experiments are significantly higher.

A method for determining a craze initiation criterion is described in Ref. [19]. Increasing the load on a spherical indenter initiates crazes in brittle polymers after reaching a critical load. The crazes develop at the edges of the indentation in radial direction. An

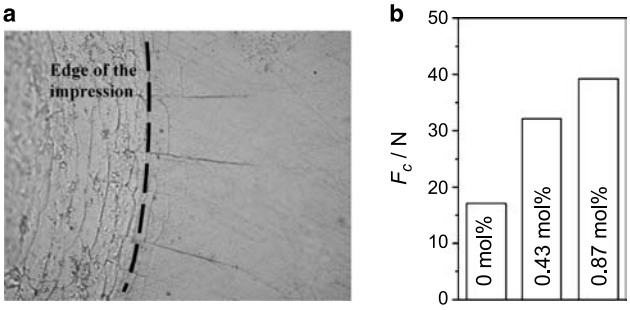

Fig. 6. Development of radial crazes at the edge of an impression (a) and dependence of the critical load for craze initiation on the cluster content (b)

example is shown in Fig. 6, where the microscopic picture of the edge region of a spherical indent is presented. During indentation, material adjacent to the indenter is pushed outwards and stresses in circumferential direction are induced. This was confirmed by numerical simulations in Ref. [19], where a maximum of hydrostatic stress was found in this edge region. The load needed for inducing crazes strongly raises with increasing cluster loading (Fig. 6). An addition of 0.87 mol% *Zr6* led to an increase of that

critical load of more than 100%. Remembering the only relatively less affected values of hardness and indentation modulus (and therefore a comparable effective strain in the different materials during the loading cycle) it can be concluded that the craze initiation stress is distinctly promoted by the clusters and the resulting cross-linking. In ongoing work we will deal with the finite element based numerical calculation of the stresses around the indenter, which could allow to determine craze initiation stress values from the critical loads and to correlate them with the network density. The influence of network density on the craze initiation stress was shown in Ref. [19] for blends of polystyrene with poly(2,6-dimethyl-1,4-phenylene oxide) (*PPO*), where the authors found an increase of this stress with increasing *PPO* content, *i.e.* network density.

One of the most important surface properties and a main topic in surface research is scratch resistance. Whereas it is difficult to evaluate the scratch resistance of polymers completely, because it depends to a large extend on materials and application parameters, micro-scratch experiments can help to understand the materials behaviour and to distinguish between different materials, already in the laboratory state.

The influence of *Zr6* loading on the micro-scratch induced deformation behaviour of the surface is presented in Figs. 7 and 8. Parameters determined to describe the geometry of the profiles obtained by scratching with constant load are shown in Fig. 7. The addition of clusters leads to a strong decrease of the pile-up height h_2 of the edge zones of the scratches. The same time the scratch depth h_1 is reduced to a large extent by the cluster loading, whereas the influence on the relative change of the scratch width parameters d_1 and d_2 is comparatively

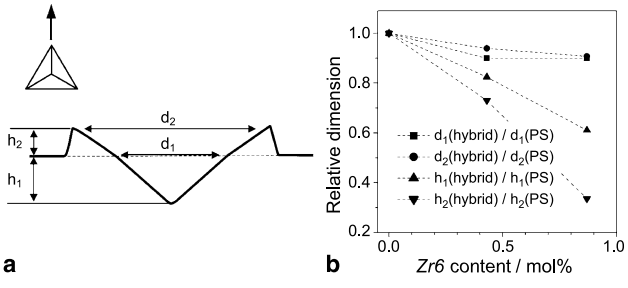

Fig. 7. Schematic cross section of a scratch (a) and dependence of the relative geometry parameters on the cluster incorporation (b)

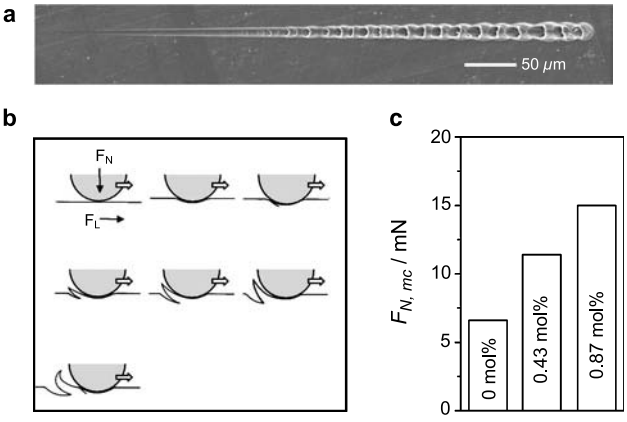

Fig. 8. Example of a scratch done by a spherical indenter with increasing normal load, material neat *PS* (a), schematic drawing of the microcracking process during scratching after [20, 21] (b), and dependence of the critical normal load for micro cracking $F_{N,mc}$ from the cluster concentration (c)

small. That means that the scratch hardness, often calculated using the parameters d_1 or d_2, is only slightly influenced by the cluster loading. Or, in other words, the scratch hardness is not suitable to describe the scratch behaviour of the investigated materials satisfactorily.

Additional information can be obtained by scratch testing with increasing load, which is a widely applied method, mainly to describe the behaviour of coated materials, but also for the characterization of surfaces of bulk materials. With this method, characteristic points in the scratch behaviour can be determined quantitatively, for example the transition from margin to plastic deformation with pile-up, the development of ploughing structures in the scratch ground or the occurrence of micro cracks in the case of brittle systems. A typical scratch trace for the investigated materials is shown in Fig. 8a. After a region of so-called margin, a more plastically deformed scratch with pile-up develops. At a critical load microcracks can be observed in the scratch ground. The process of the development of these microcracks are described by *Yang* and *Wu* [20, 21] and shown schematically in Fig. 8b. From the critical load $F_{N,mc}$ a craze break-down stress can be calculated [20, 21].

There is a strong increase of the critical load for craze breakdown with increasing cluster content (Fig. 8c). This increase is much higher than the increase in indentation hardness. Because the development of microcracks is mainly influenced by the tensile deformation behaviour of the materials these

results show again the larger influence of cluster loading on the tensile properties when compared to the compression properties.

Conclusion and Outlook

The mechanical properties of hybrid polymers, which were prepared by a step-wise co-polymerization of styrene and different proportions of the multifunctional zirconium oxo cluster $Zr_6O_4(OH)_4$(methacrylate)$_{12}$ were investigated with focus on the surface mechanical properties. Whereas the indentation hardness, indentation modulus and indentation creep behaviour are relatively slightly influenced by the cluster concentration, a strong increase of craze initiation load and of the critical load for craze breakdown, *i.e.* opening of microcracks, was observed by ball indentation and micro scratch experiments. The materials behaviour detected by indentation methods correlates to the behaviour in uniaxial tensile and compression loading and can be ascribed to the cross-linking by the *Zr6* clusters.

In ongoing and future work the results will be combined with finite element simulation work. Then critical stresses and strains for the initiation and the break down of crazes can be calculated, which would help to describe the deformation behaviour of the organic-inorganic hybrid materials more accurately. Additionally, the creep experiments have to be extended. The strains can be varied by applying different loads leading to a variation of the indentation depths. Furthermore, viscoelastic models have to be applied to determine viscosity values from the creep curves. So, the description of the mechanical behaviour of the materials by indentation methods can be completed.

Experimental

Methods

Dynamic Mechanical Analysis (DMA) was performed with a TA Instruments DMA 2980 in tension mode at a frequency of 1 Hz and a heating rate of 2 K/min. The sample size was 15 mm × 5 mm × 0.5 mm and a dynamic amplitude of 0.1% was applied.

Tensile and compression tests were carried out on a Zwick Z050 universal testing machine. For the tensile measurements dog-bone-shaped specimens with a geometry of 35 mm × 2 mm × 0.5 mm according to ISO 527-2 were produced. The clamp length was 20 mm and the cross-head speed 0.5 mm/min. Cylindrical specimens with a height of 6 mm and a diameter of 4 mm were used for the compression tests. The strain rate was $0.013\,s^{-1}$. To reduce the friction a thin *PTFE* tape and a lubricant were placed between the samples and the steel plates [16].

Indentation testing was performed at different load scales. Microhardness measurements were done using a Nanoindenter XP, MTS Systems, with a constant indentation rate of 100 nm/s to a maximum indentation depth of 2 μm. At this depth the load was kept constant for 30 s, followed by unloading. The indentation hardness was determined as described in [22, 23]. From this unloading segment the indentation modulus was calculated according to ibidem.

The indentation creep tests were carried out using a rounded conical tip having a tip radius of 4.7 μm. A load of 10 mN was applied within 3 s and then hold constant for 300 s. According to [22] an indentation creep parameter C_{IT} can be calculated using Eq. (1).

$$C_{IT} = \frac{h_2 - h_1}{h_1} \times 100\%, \tag{1}$$

with h_1 . . . indentation depth at the time of reaching the test force, h_2 . . . indentation depth at the end of the holding time.

To look more inside the indentation creep behaviour, viscoelastic contact models have been applied to creep problems [18]. For a spherical indenter with the radius R there exists the relationship (2) between the creep compliance $J(t)$, the constant load F_0, the contact area $A(t)$ and the indentation depth $h(t)$ [18]:

$$J(t) = \frac{8h(t)\sqrt{A(t)}}{3\sqrt{\pi}(1-\nu)F_0} \tag{2}$$

Equation (2) was simplified with the assumption that the *Poisson* ratio ν remains constant.

For the observation of the craze initiation behaviour an Emco M1C010/100 hardness tester, equipped with an 1 mm diameter steel sphere, was used. To obtain this critical load the applied load was increased stepwise by 1 N. The load where the first crazes or microcracks occur at the edge of the impressions was determined as the crack initiation load.

Using the nanoindentation device scratch tests can be performed. The scratch testing was done in two ways, with constant load and with linear increasing normal load. In the case of the constant load scratch tests a Berkovich indenter, loaded with 10 mN, was moved edge on through the material. After 1 day the geometry of the remaining scratches was measured using a scanning force microscope PSIA XE-100 in semi-contact mode. The scratch tests with linear increasing load were done with the rounded conical tip (radius 4.7 μm). The normal load was increased from 0 to 20 mN, the rate was 2 mN/s. In all cases the lateral scratch velocity was 50 μm/s.

Acknowledgements

U. Schubert and *F.R. Kogler* thank the Fonds zur Förderung der wissenschaftlichen Forschung (FWF) for financial support of the work.

References

[1] Schubert U (2001) Chem Mater **13**: 3487
[2] Kogler FR, Jupa M, Puchberger M, Schubert U (2004) J Mater Chem **14**: 3133
[3] Fanovich MA, Pellice SA, Galliano PG, Williams RJJ (2002) J Sol Gel Sci Tech **23**: 45
[4] Martinez Urreaga J, Matias MC, Lorenzo V, de la Orden MU (2000) Mater Lett **45**: 293
[5] Zheng M, Gu M, Jin Y, Jin G (2000) Mater Sci Eng B **77**: 55
[6] Mammeri F, Rosez L, Sanchez C, Le Bourhis E (2003) J Sol Gel Sci Tech **26**: 413
[7] Mammeri F, Le Bourhis E, Rozes L, Sanchez C, Huignard A, Levefre D (2004) J Non Cryst Sol **345** and **346**: 610
[8] Perrin FX, Nguyen VN, Vernet JL (2002) Polym Int **51**: 1013
[9] Mammeri F, Le Bourhis E, Rozes L, Sanchez C (2005) J Mater Chem **15**: 3787
[10] Huang J, He C, Liu X, Xu J, Tay CSS, Chow Y (2005) Polymer **46**: 7018
[11] Innocenzi P, Esposto M, Maddalena A (2001) J Sol Gel Sci Tech **20**: 293
[12] Perrin FX, Nguyen VN, Vernet JL (2002) Polymer **43**: 6159
[13] Gao Y, Kogler FR, Schubert U (2005) J Polym Sci A **43**: 6586
[14] Kogler FR, Koch T, Peterlik H, Seidler S, Schubert U (2006) J Polym Sci B, submitted
[15] Kogler FR (2005) PhD Thesis, TU Vienna
[16] Van Melick HGH, Govaert LE, Meijer HEH (2003) Polymer **44**: 2493
[17] O'Connor KM, Cleveland PA (1993) Mater Res Soc Symp Proc **308**: 495
[18] Vanlandingham MR, Chang NK, Drzal PL, White CC, Chang SH (2005) J Polym Sci Phys **43**: 1794
[19] Van Melick HGH, Bressers OFJT, den Toonder JMJ, Govaert LE, Meijer HEH (2003) Polymer **44**: 2481
[20] Yang ACM, Wu TW (1993) J Mater Sci **28**: 955
[21] Yang ACM, Wu TW (1997) J Polym Sci Phys **35**: 1295
[22] ISO 14577 (2002)
[23] Oliver WC, Pharr GM (1992) J Mater Res **7**: 1564